

Robots Taking Initiative in Collaborative Object Manipulation: Lessons from Physical Human-Human Interaction

Zhanibek Rysbek^{1*}, Ki Hwan Oh^{1*}, Afagh Mehri Shervedani¹, Timotej Klemenčič², Miloš Žefran¹, and Barbara Di Eugenio³

Abstract—Physical Human-Human Interaction (pHHI) involves the use of multiple sensory modalities. Studies of communication through spoken utterances and gestures are well established, but communication through force signals is not well understood. In this paper, we focus on investigating the mechanisms employed by humans during the negotiation through force signals, and how the robot can communicate task goals, comprehend human intent, and take the lead as needed. To achieve this, we formulate a task that requires active force communication and propose a taxonomy that extends existing literature. Also, we conducted a study to observe how humans behave during collaborative manipulation tasks. An important contribution of this work is the novel features based on force-kinematic signals that demonstrate predictive power to recognize symbolic human intent. Further, we show the feasibility of developing a real-time intent classifier based on the novel features and speculate the role it plays in high-level robot controllers for physical Human-Robot Interaction (pHRI). This work provides important steps to achieve more human-like fluid interaction in physical co-manipulation tasks that are applicable and not limited to humanoid, assistive robots, and human-in-the-loop automation.

I. INTRODUCTION

Collaborative object manipulation involves many sensory modalities, including gestures, body posture, eye gaze, and force exchanges. Humans often use different modalities to express their intent or devise an action plan. During Activities of Daily Living (ADL), partners usually plan ahead before engaging in a dyadic task. However, the plans are not always complete and the dyads sometimes need to resolve conflicts or miscommunication during the execution of the task. For example, dyads may discuss where approximately to relocate the dining table but omit details such as the final orientation of the table, or how to navigate the table around other furniture in the room. Such remaining details are typically resolved by employing one or more sensory modalities during the execution of the task. While we have tools to interpret spoken utterances and gestures [1], communication through force signals is not well-studied. But given that humans routinely communicate that way, robots need

Collaborative Object Relocation

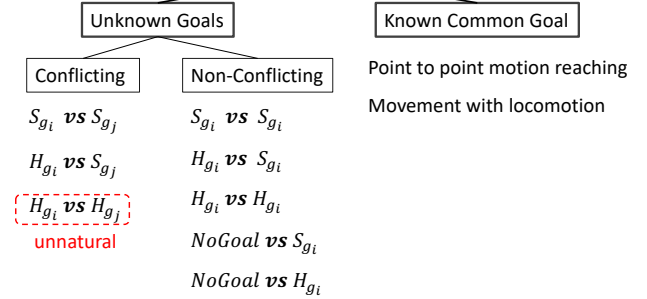


Fig. 1. Goal taxonomy for collaborative object relocation. Subscript g_i represents soft goal to a goal direction g_i ($i \neq j$).

to have the capability to both understand force signals and express their intent through them if they are to engage in human-like physical interaction.

Negotiating to reach a consensus is an integral part of successful collaboration. Quite often, literature on HRI assumes that a robot plays a subordinate role to the human in collaborative tasks. A widely used paradigm for such applications is programming by demonstration [2]–[4] that formulates human behavior as repeatable actions. Robot response is often modulated by impedance control or admittance control [5], [6]. On the other hand, aspects of human-human interactions are studied by haptics and kinematic metrics in virtual environments [7]–[9]. Authors in [10], propose a model that computes interaction force for ballistic motions, where trajectory closely follows minimum jerk [11]. Human-robot interaction strategies are studied by distinguishing different haptic cues [12]. In recent work, [13] proposed a pHRI system with the ability to detect conflicts based on the metrics suggested in [14]. Given the scant existing work, our focus is on force communication, and in particular the mechanisms employed by the humans during the negotiation through force signals. It is only after we have a good understanding of human behavior that we can hope to design robots that can imitate us.

To explore force communication mechanisms that humans exploit, we ground our study on a collaborative relocation task with uncertain goals that require active communication over a haptic medium. The rest of the paper is structured as follows: in Section II, we present the taxonomy that categorizes human behaviors conditioned on the available task-related information. Then, in Section III we describe a human study experiment during which participants negotiate a direction following each category in the taxonomy. In Sec-

* First two authors contributed equally to this work.

¹Z. Rysbek, K.H. Oh and Miloš Žefran are with the Robotics Lab, Department of Electrical and Computer Engineering, the University of Illinois at Chicago, Chicago, IL 60607, USA.

²T. Klemenčič is with the Laboratory of Robotics, Faculty of Electrical Engineering, University of Ljubljana

³B. Di Eugenio is with the Natural Language Processing Lab, Department of Computer Science, the University of Illinois at Chicago, Chicago, IL 60607, USA.

This work has been supported by the National Science Foundation grants IIS-1705058 and CMMI-1762924.

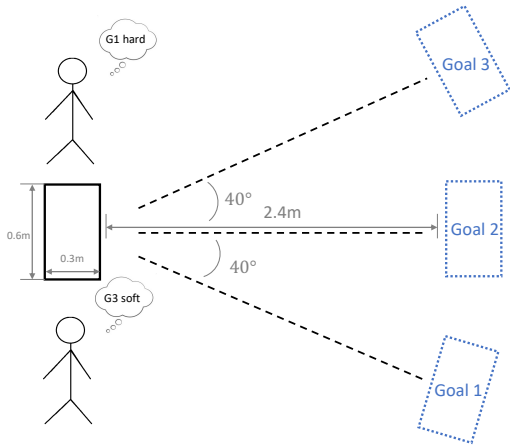


Fig. 2. Experimental Environment

tion IV, we propose and discuss features designed to detect and describe human intent based on force-kinematic signals. Section V presents the statistical correlation of categories in the taxonomy based on how fast dyads reach a consensus, discusses the discriminating capacity of the proposed features from the human-human data, and demonstrates the feasibility of intent classification by clustering analysis. Finally, Section VI summarizes the contribution of this paper with implications for future work.

II. DYADIC GOAL TAXONOMY

When dyads engage in a manipulation task, spatial awareness is a key aspect of the interaction, as they must know where to move. Considering this, we take an approach that partners always start either with a preferred goal direction in mind or with no preference at all. Without loss of generality, if there are N potential goal locations, each agent's goal is $g_k \in \{NoGoal, 1, 2, \dots, N\}$, $k = 1, 2$, where k is the agent number. *NoGoal* implies a follower role.

Moreover, we observed different levels of commitment to a chosen goal direction by dyads from our previous work [15]. One partner that is more committed to its goal leads and dominates the interaction, or vice versa, a less committed partner tends to agree by compromising their intent. In daily life, such situations occur when a person who has a better view of the obstacles is likely to lead. In order to model the variations of commitment, we introduce *hard* and *soft* goal configuration. *Hard* goal configuration requires the subject to go to the assigned goal position and they have to convince the partner to comply even if they disagree. Whereas, *soft* goal configuration means that the goal would be the preferred location if no opposition is recognized from the partner. We note that this would be an example of dynamic leader-follower behavior, although it differs from what is typically studied in the literature [10], [16], [17].

Fig. 1 summarizes all possible goal combinations for the agents. In the hierarchy of the goals, we have **unknown goal** (UG) and **Known Common Goal** (KCG). KCG represents the case when partners explicitly talk about the intended goal before starting the task and the final goal configuration is agreed upon. This type of interaction does not have

an explicit directional negotiation. An example of KCG cases is point-to-point motions with/without locomotion. The trajectory of the object is similar to minimum jerk trajectories [10], [11]. In UG cases, however, partners do not know each other's intended goals. Therefore, interactions can evolve into **conflicting** and **non-conflicting** scenarios. Depending on the level of commitment there could be 5 unique non-conflicting cases without repetitions (Fig. 1). Unlike in KCG, dyads take extra time to perceive the intent of the partner as it is not clear if both have the same goal or not.

Conflicting interactions may unfold in 3 unique cases. In conflicting *hard vs soft* goal configurations, interaction unfolds in the favor of a *hard* goal dyad. However, conflicting *soft vs soft* interaction is prone to be dynamic as both partners are equally committed to different goals, and interaction may take longer. In this case, force exchange may take more back-and-forth turns before the conflict is resolved. In the *Hard vs Hard* case with conflicting goals, the conflict can not be resolved since both agents may refuse to compromise. We will therefore not study such interactions further.

An important motivation for this work is to explore conflicting UG scenarios that are less studied in the literature. Many of the existing studies focus on reaching motions [10] and motions with locomotion [2] that can be classified as KCG (see Fig. 1). Interaction state classifier in [13] detects conflicting or non-conflicting states, which allowed the robot to switch to proactive collaboration in non-conflicting instances, and switched back to a passive follower when conflict is encountered. This interaction scenario can be thought of as a special case of the goal taxonomy where the robot starts with *NoGoal* preference and the human partner has a clear goal direction in mind (*NoGoal vs Soft* or *NoGoal vs Hard*). We are especially interested in the *Soft vs Soft* interactions, as both partners are equally committed to their goals, have no knowledge of the partner's intent, and are willing to compromise their intent based on the partner's action. At the same time, such goals assigned to subjects elicit active negotiation and provide valuable pHRI data. In the remainder of the paper, we will thus focus on the conflicting UG interactions.

III. EXPERIMENT

A. Task

An experiment was designed to study directional decision-making in physical human-human interaction. A diagram of the environment is shown in Fig. 2. The task is to collaboratively relocate the tray to one of three goal locations ($N = 3$). Goal locations are spread out in a circular manner, where the radius is approximately 2.4m with 40° angular spacing. Before the start, each subject privately receives randomly assigned goal configuration g_k where $g_k \in \{NoGoal, S_i, H_i\}$, $k = 1, 2$, $i = 1, 2, 3$. Subjects were instructed to only communicate through the haptic sense, and they are prohibited to chat, use gestures, or make eye contact. Moreover, they were asked to grasp firmly with the comfortable hand that keeps the body open during the maneuver. Two beep sounds are generated to control the

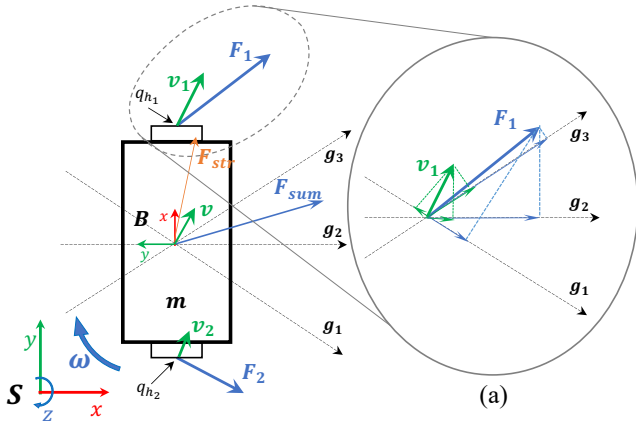


Fig. 3. Free body diagram of the manipulated object in a relocation task. S - ground fixed spatial frame, B - body affixed frame, m - object mass, v - velocity of the center of mass, v_1, v_2 - velocities of handle 1 and 2 respectively, F_1, F_2 - applied forces, ω - object rotational velocity, g_1, g_2, g_3 - goal directions, q_{h1}, q_{h2} are grasping points. (a) Example of the projection of force and velocity to goal directions.

initial movements. The first beep signals the time to grasp the tray, and the second beep permits them to move in the assigned direction. This allows us to measure the grasping force when they are static between the beeps and the exact initial time of the negotiation phase. Subjects engage in negotiations either to convince them to follow their goal or to give up their assigned goal. After delivering the object to the goal location, they follow the same procedure to come back to the initial position. However, there is no explicit directional decision since they both clearly know the final destination. Therefore, it can be labeled as a KCG goal from Fig. 1.

The experiment was conducted across 4 days, and a total of 16 subjects were recruited from the University of Illinois at Chicago campus. In a single day, 4 participants formed 6 dyads, summing 24 dyads across 4 days. Before engaging in the task, they were given time to practice adapting to the beeps and learn the goal types. This alleviates the learning effect. The human study experiment was conducted according to IRB protocol.

B. Setup

A wooden tray is used as a manipulated object. To track the interaction we have attached two RFT60 force-torque sensors between the handle and the tray (Robotous Inc.). 6-DOF IMU sensor was used to track the linear acceleration and the angular velocity. Both, IMU and force-torque sensors are connected to an onboard Raspberry Pi that wirelessly transmitted the data to the main computer in real-time. The sampling rate for the force-torque sensor was 200Hz, and for the IMU was 100Hz. Including onboard equipment weight of the tray was 2.3kg and the dimensions were 61cm \times 31cm. The 6D pose of the tray was tracked using the ArUco library from OpenCV [18]. Several fiducial markers were attached to the surface and the sides of the tray. To deal with occlusions, three cameras overlooking the experimental environment recorded the image streams and transmitted them to the main

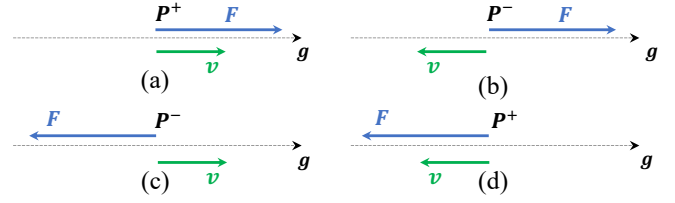


Fig. 4. Combination of the signs of force and velocity and resulting power.

computer with a USB cable. Robot Operating System (ROS) is used as a data collection environment.

Extended Kalman Filters [19] are used to fuse angular velocity and orientations from three cameras. Subsequently, position and velocity signals were obtained using linear Kalman Filters by fusing linear acceleration and position data. All signals including force-torque, pose, twist, and accelerations were pre-processed using a low-pass filter with a cutoff frequency of 12.5Hz.

IV. DELIBERATE ACTION METRICS

A. Force communication

It is widely accepted that dyads communicate with force exchanges in haptically-coupled tasks. The consequence of two agents trying to move the same object results in exerting excessive effort more than what it takes to move the object. That is, $|F_{sum}| \leq |F_1| + |F_2|$, where F_1, F_2 are forces each agent applied and $F_{sum} = m\ddot{x} = F_1 + F_2$.

The interaction force is the excessive component of applied force that does not contribute to the motion. Knowing the precise interaction force can tell us about the accurate state of the interaction. However, existing approaches that compute this force cannot be used for deliberate locomotions [7], [10], [20]. In our task, we are interested in finding the human intent during general walking motions. This adds many confounding components of interaction force such as varying grasping force and oscillation due to walking. This increases the signal-to-noise ratio and makes it difficult to estimate the clear intent of the dyads. While grasping force can be estimated at the rest moments such as the start and the end instances of the interaction, it is not feasible to estimate it during the motion [14]. Therefore, additional kinematic signals are required to interpret the human intent, unlike the haptic-only approach in [13].

B. Interaction Power

Dyads use push and pull actions creating temporal conflict to express their intent. This causes a sharp rise in the magnitude of the difference of the forces ($F_1 - F_2$) [15]. The attitude toward this phenomenon varies in the literature. For example, authors in [7] and [21] regard avoiding the conflict as merely an objective of the dyads, and the force of the agent who is not contributing to the motion is considered as the interaction force. In contrast, based on human experiments, we view temporal conflict as the consequence of symbolic actions in a conflicting goal direction. Hence, the key to interpreting agent intent is to look at the periods of such

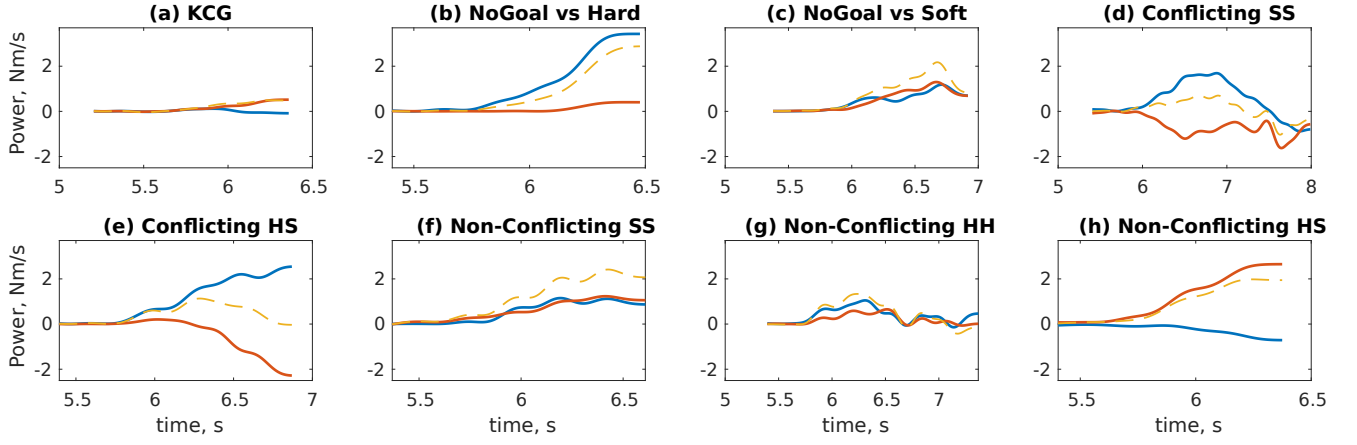


Fig. 5. Examples of power index from experimental observations by interaction types. Respective interaction types are shown on the title of the subplots. Power by subject 1 and subject 2 are denoted with blue and red curves respectively. The yellow dashed curve represents the sum of the power applied to the center of the mass.

actions. An important observation is push-pull actions result in slight movement in the object. Thus, we propose to refer to the instantaneous power of each agent:

$$P_k(t) = F_k \cdot v_k = \|F_k\| \|v_k\| \cos(\angle(F_k, v_k)) \quad k = 1, 2 \quad (1)$$

where k denotes the agent number. The velocity of the grasping point v_k is measured as follows.

$$v_k^s = R_{sb} \cdot (\omega_b \times q_k^b) + \dot{p}_{sb}, \quad k = 1, 2 \quad (2)$$

where v_k^s denotes the velocity of handle k in the spatial frame (Fig. 3), q_k^b and ω_b are the handle position and the angular velocity expressed in body frame \mathbf{B} (center of the tray), R_{sb} and \dot{p}_{sb} are the rotation matrix and the velocity of frame \mathbf{B} relative to spatial frame \mathbf{S} (global reference frame) respectively. Analogously, total exerted power on the object can be computed as:

$$P_{sum}(t) = F_{sum} \cdot v = \|F_{sum}\| \|v\| \cos(\angle(F_{sum}, v)) \quad (3)$$

where v is the velocity of frame \mathbf{B} . Similar metrics exist in the literature, where authors in [9], [22] use power in a scalar form to distinguish interaction patterns in the virtual environment.

Note that, positive power implies that the agent is applying force in the direction of velocity which contributes to the motion significantly. Negative power implies that the person is resisting the motion. In the context of interaction, this could be accepted as opposition. Examples from the experiment are discussed in Section V.

C. Power to Goal directions

The interaction power is suitable to determine the general direction of motion. However, the symbolism of the action is tied to the valid goal direction. One such way to interpret agent action is to look at the projection of the power in goal directions. Hence, exerted power by an agent reflected in a goal direction g_i can be defined as:

$$P_k^{g_i} = F_k^{g_i} \cdot v_k^{g_i} = \|F_k\| \|v_k\| \cos(\angle(F_k, g_i)) \cos(\angle(v_k, g_i)) \quad (4)$$

And projected force and velocity for each agent k are defined as follows:

$$F_k^{g_i} = \|F_k\| \cos(\angle(F_k, g_i)) \quad (5)$$

$$v_k^{g_i} = \|v_k\| \cos(\angle(v_k, g_i)) \quad (6)$$

Note that both $F_k^{g_i}$ and $v_k^{g_i}$ are scalar quantities. When an agent applies force in a particular direction, the respective projection of the force will resonate (see Fig. 3a to goal 1). Likewise, opposition to the motion is reflected as a negative force in a goal direction (Fig. 3a to goal 3). Power represents the manifestation of the action in a direction. Because, when there is a movement – power is non-zero. It is important to note, that positive projected power does not always represent a positive effort to a goal (see Fig. 4) because negative force and velocity will result in the positive power as shown in Fig. 4d. Although, in the latter case it symbolically means moving away from that goal.

V. RESULTS AND DISCUSSION

A. Negotiation phase and Goal Taxonomy

The decision-making phase in a task happens at the beginning of the motion. And it ends when agents settle into a common direction after the active negotiation phase [15]. Force exchanges applied beyond the negotiation phase are irrelevant to directional decision-making and are detrimental in identifying actions related to major decisions. Hence, it is crucial to find the precise boundary of the negotiation phase for meaningful analysis. Beep times give us the exact moment when subjects initiate the motion, but the end time of the negotiation phase must be estimated from the data. By definition, the negotiation phase ends when subjects resolve the conflict. This implies that the direction of the object's velocity is heading toward the goal during the execution phase. One way to estimate that is as follows:

$$t_{dec} : \text{dist}(p(t) + \lambda v(t), l(g)) < \varepsilon, \quad \forall t \geq t_{dec}, \quad \lambda \in \mathbb{R} \quad (7)$$

where $p(t) + \lambda v(t)$ is the line defined by the object coordinate $p(t)$ and velocity $v(t)$, $l(g)$ is the coordinate of goal g , and

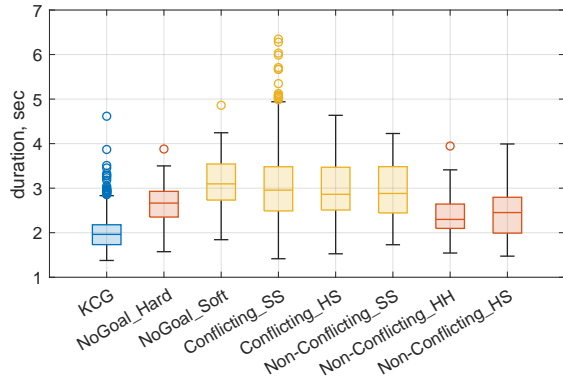


Fig. 6. Box chart of negotiation phase duration by 8 different goal assignment combinations. Points outside of whiskers are outliers. Box represents the 25th and 75th percentile. Different colors represent grouping by statistical similarity.

TABLE I
CLUSTERING SCORES

Assigned Goal	Calinski-Harabasz	Davies-Bouldin	Silhouette
H1	289.5661	0.9207	0.5187
H2	195.1549	0.6994	0.5650
H3	309.7367	0.7544	0.5682

$dist$ is function between the line and a point. Threshold ϵ can be different depending on the scale of the environment. In our experiment, $\epsilon = 0.2m$ was chosen and the negotiation time is measured as $t_{dec} - t_{start}$.

Fig. 6 illustrates the box chart of the negotiation time from each interaction type described in Section II. According to ANOVA results, KCG dyads spent the least amount of time for negotiation compared to all the other interactions ($p < 0.038$). This is expected since in UG cases subjects take extra time to perceive their partner’s intent and increase the time to settle into a common goal. Negotiation time for *NoGoal vs Hard*, *Non-Conflicting HH*, and *Non-Conflicting HS* were significantly different from *NoGoal vs Soft* and *Conflicting SS* ($p < 0.005$). And during *Conflicting HS* dyads negotiated longer compared to *Non-Conflicting HH* and *Non-Conflicting HS* ($p < 0.003$). Tukey’s honestly significant difference test was used to estimate pairwise differences. One can note that non-conflicting interactions involving one *Hard* goal subject (red boxes) have a shorter mean value. This can be explained by the presence of a decisive agent that simplifies the decision-making process. Whereas, conflicting interactions (yellow boxes in Fig. 6) have larger mean values compared to the rest. Since both partners are equally committed to their goal, interaction might take a few more turns compared to the *Hard* goal case.

Fig. 5 shows power indices measured during the negotiation phase for each type of interaction. During the KCG case, dyads do not negotiate major directions. Consequently, the magnitude of applied forces and power remains low compared to UG cases. Fig. 5a shows a KCG case where both subjects moved simultaneously to the goal. In some cases, KCG might resemble conflicting interactions due to

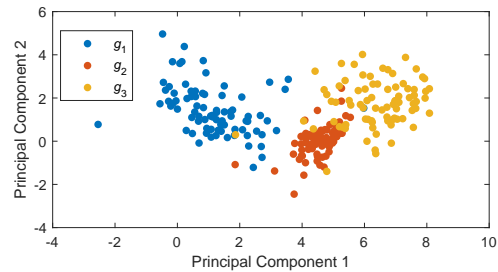


Fig. 7. Strength of intent projected to 3 goals in all interactions where an agent had goal H3. The data is well clustered after LDA dimensionality reduction to two principal components.

delayed response. But, common traits are fast acceleration and sustained velocity of the object in the goal direction.

Non-conflicting interactions share similar patterns where both subjects cooperate to the same motion and $P_{sum} = |P_1| + |P_2|$ holds true (Fig. 5f,g,h). However, the level of commitment might change the picture. For example, in Fig. 5h a subject assigned to *Hard* goal (red) moved more aggressively leaving the partner behind, although *Soft* goal subject (blue) did not show clear opposition.

Follower mode situations are shown in Fig. 5b and c respectively against *Hard* and *Soft* (leader) goals. Note that, the power of the follower agent in the former case is around zero and *hard* goal dominates the motion. In contrast, *soft* goal case both of them similarly exert effort, which indicates the proactive behavior of the follower.

Conflicting HS in Fig. 5e shows the situation where each partner with a different intention actively moves in the opposing direction causing significant conflict. Typically, bifurcation is observed from power plots where directional disagreement (explicit negotiation) occurs. Then, the subject with the *hard* goal assignment (blue) drags the object with extra force, and the object travels in its direction.

Among all possible interaction types, *conflicting SS* is the most dynamic. The real action of the subject with a *Soft* goal varies from giving up the assigned goal too easily or exerting too much effort. Hence, a number of *conflicting SS* interactions might resemble similar patterns as in the rest of the interaction types. However, *conflicting SS* contains unique situations where subjects take more turns to resolve the conflict assuming the partner can change their mind. Fig. 5d shows an example where both partners initially opposed each other causing significant bifurcation, but subject 2 (red) decides to concede afterward.

B. Action identification

The main challenge in an application like ours is detecting individual actions in a time-dependent signal. To detect push-pull actions we exploit patterns in the power signal. When an agent exerts significant force causing the object to move it creates peak shapes in power signals. In this work, we devised an action detection algorithm in a similar fashion as in [15]. Specifically, we focus on the rising edge of the peak in the power signal. A peak associated with the action

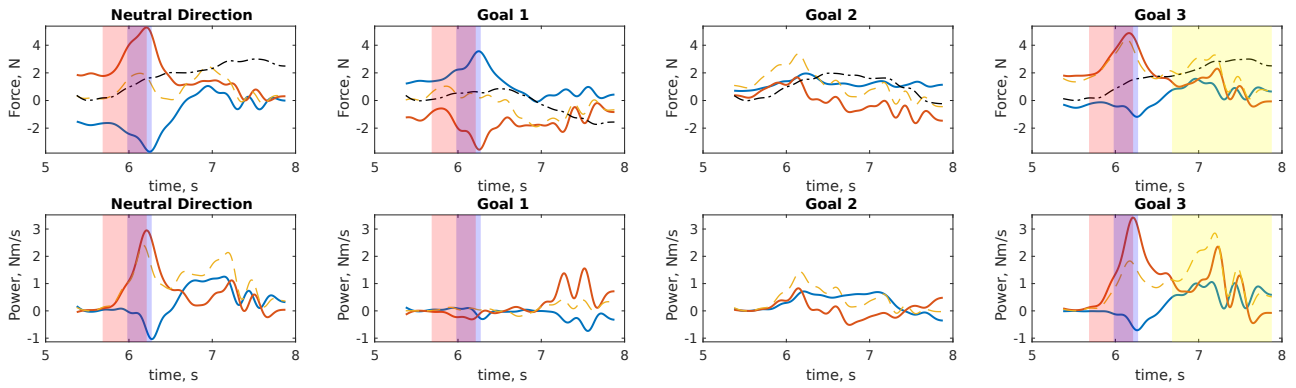


Fig. 8. Force, velocity, and power and their projection to goal directions. Force and velocity are shown in the first row, and the power is in the second. Subject 1 and subject 2 are denoted in blue and red curves respectively, the yellow dashed curve is the sum of the force (first row) and power (second row). The black dashed curve is scaled velocity. Blue and red shaded areas represent the action periods for subjects 1 and 2 respectively. The yellow-shaded area is the execution phase. In this example, subject 1 was assigned to S_1 and subject 2 to S_3 .

is determined by the spatiotemporal filter. As a temporal constraint, human reaction time for touch stimulus (0.15s) [23] and simple reaction time (0.25s) [24] were considered.

An example of action detection is shown in Fig. 8. The algorithm identified action regions shaded in blue and red for subjects 1 and 2. In the power plot (bottom left), subject 2 made a significant effort to cause the object to move. Subject 2 (blue) showed little opposition with a short delay. After the shaded area, tension decreases and follows to the execution phase. When the power in the neutral direction is seen in a different goal direction, it is clear that actions behind this movement were intended in towards goal 3 (Fig. 8 lower right). Although subject 1 managed to apply opposing force which did not cause a motion, the power signal in goals 1 and 2 remained low. Thus, individual actions and their intended goal directions are interpreted.

As mentioned in Section IV, force components due to grasping and walking interferes with the direction of pull and create ambiguity in identifying the intended goal direction. That is, maximum power among projected goal directions is not necessarily the intended goal. This problem can be solved as a classification problem by aggregating features extracted from force, velocity, and power signals from the action phase. Fig. 7 demonstrates the clusterability of the intended direction for all interactions involving *hard* goal 3. Table I, reports the clustering score for H1, H2, H3 cases. Therefore, we show the feasibility of interpreting symbolic events from the force-kinematic signals.

VI. CONCLUSION

This work attempts to address an important problem in human-robot co-manipulation where dyads actively communicate with force signals. The task is grounded on a realistic world scenario where participants decide to move an object collaboratively to an uncertain goal. A taxonomy is presented that captures the diversity of human behavior conditioned on how much each participant possesses task-related information and extends human-human interaction scenarios studied in the literature. Based on that the human study experiment

was designed. We emphasize that interactions that involve unknown goals are the least studied in robotics research. Therefore, we skewed the distribution of corresponding cases in the experiment. Empirical analysis of negotiation time shows the statistical significance of different categories of the taxonomy.

Furthermore, we observed due to the delay in reaction, the participants seem to communicate and express intent in epochs. To identify such human intents we propose novel features derived from force-velocity signals. Presented features are designed to accommodate arbitrary locations and numbers of goals, crucial for robot functionality in unstructured and changing environments. Additionally, projected features allow the mapping of low-level signals into symbolic action – input to a high-level reasoning module. A preliminary analysis of proposed features demonstrates discriminating capacity where the corresponding feature resonates consistently when a participant shows intent.

The overarching goal of this research is to develop a high-level robot controller that can physically collaborate with humans by taking the human lead as well as taking initiative when needed. This necessitates 3 major components of the controller: (1) the ability to understand human intent, (2) clearly express its own intent and (3) action policy that reaches the consensus. The clustering analysis presented in this paper demonstrates the feasibility of training a classifier to recognize human intent in real-time (component 1). The future continuation of this research involves designing a real-time human intent classifier and high-level robot controller with human intent feedback.

The ability of humans to engage in a vast diversity of collaborative tasks sets high expectations for robots to be used in daily life. Robots that lack human interactive controllers have much less use in practice. Therefore, the authors believe this work contributes to filling the gap in the literature to attain more fluid human-robot interaction. The application of such systems is vital in practice ranging from humanoids, assistive robots, rehabilitation, and human-in-the-loop automation.

REFERENCES

- [1] B. Abbasi, N. Monaikul, Z. Rysbek, B. D. Eugenio, and M. Žefran, “A Multimodal Human-Robot Interaction Manager for Assistive Robots,” in *2019 IEEE/RSJ International Conference on Intelligent Robots and Systems (IROS)*, Nov. 2019, pp. 6756–6762.
- [2] J. Campbell, S. Stepputtis, and H. Ben Amor, “Probabilistic Multimodal Modeling for Human-Robot Interaction Tasks,” in *Robotics: Science and Systems XV*. Robotics: Science and Systems Foundation, Jun. 2019.
- [3] A. D. Dragan, K. Muelling, J. Andrew Bagnell, and S. S. Srinivasa, “Movement primitives via optimization,” in *2015 IEEE International Conference on Robotics and Automation (ICRA)*. Seattle, WA, USA: IEEE, May 2015, pp. 2339–2346.
- [4] A. Billard, S. Calinon, R. Dillmann, and S. Schaal, *Robot Programming by Demonstration*. Berlin, Heidelberg: Springer Berlin Heidelberg, 2008, pp. 1371–1394. [Online]. Available: https://doi.org/10.1007/978-3-540-30301-5_60
- [5] N. Hogan, “Impedance Control: An Approach to Manipulation: Part I—Theory,” *Journal of Dynamic Systems, Measurement, and Control*, vol. 107, no. 1, pp. 1–7, 03 1985. [Online]. Available: <https://doi.org/10.1115/1.3140702>
- [6] L. D. Roza, S. Calinon, D. Caldwell, P. Jimenez, and C. Torras, “Learning Collaborative Impedance-Based Robot Behaviors,” in *Twenty-Seventh AAAI Conference on Artificial Intelligence*, Jun. 2013. [Online]. Available: <http://www.aaai.org/ocs/index.php/AAAI/AAAI13/paper/view/6243>
- [7] R. Groten, D. Feth, H. Goshy, A. Peer, D. A. Kenny, and M. Buss, “Experimental analysis of dominance in haptic collaboration,” in *RO-MAN 2009 - The 18th IEEE International Symposium on Robot and Human Interactive Communication*, 2009, pp. 723–729.
- [8] A. Mörtl, M. Lawitzky, A. Kucukyilmaz, M. Sezgin, C. Basdogan, and S. Hirche, “The role of roles: Physical cooperation between humans and robots,” *The International Journal of Robotics Research*, vol. 31, no. 13, pp. 1656–1674, Nov. 2012. [Online]. Available: <http://ijr.sagepub.com.proxy.cc.uic.edu/content/31/13/1656>
- [9] C. E. Madan, A. Kucukyilmaz, T. M. Sezgin, and C. Basdogan, “Recognition of haptic interaction patterns in dyadic joint object manipulation,” *IEEE Transactions on Haptics*, vol. 8, no. 1, pp. 54–66, 2015.
- [10] E. Noohi, M. Žefran, and J. L. Patton, “A model for human–human collaborative object manipulation and its application to human–robot interaction,” *IEEE transactions on robotics*, vol. 32, no. 4, pp. 880–896, 2016.
- [11] T. Flash and N. Hogan, “The coordination of arm movements: an experimentally confirmed mathematical model,” *Journal of neuroscience*, vol. 5, no. 7, pp. 1688–1703, 1985.
- [12] J. Dumora, F. Geffard, C. Bidard, T. Brouillet, and P. Fraisse, “Experimental study on haptic communication of a human in a shared human-robot collaborative task,” in *2012 IEEE/RSJ International Conference on Intelligent Robots and Systems*, 2012, pp. 5137–5144.
- [13] Z. Al-Saadi, Y. Hamad, Y. Aydin, A. Kucukyilmaz, and C. Basdogan, “Resolving conflicts during human-robot co-manipulation,” 01 2023.
- [14] E. Noohi and M. Zefran, “Quantitative measures of cooperation for a dyadic physical interaction task,” in *Humanoid Robots (Humanoids), 2014 14th IEEE-RAS International Conference on*. IEEE, 2014, pp. 469–474.
- [15] Z. Rysbek, K. H. Oh, B. Abbasi, M. Žefran, and B. Di Eugenio, “Physical action primitives for collaborative decision making in human-human manipulation,” in *2021 30th IEEE International Conference on Robot & Human Interactive Communication (RO-MAN)*, 2021, pp. 1319–1325.
- [16] A. Thobbi, Y. Gu, and W. Sheng, “Using human motion estimation for human-robot cooperative manipulation,” in *2011 IEEE/RSJ International Conference on Intelligent Robots and Systems*, Sep. 2011, pp. 2873–2878.
- [17] A. Tsiamis, C. K. Verginis, C. P. Bechlioulis, and K. J. Kyriakopoulos, “Cooperative manipulation exploiting only implicit communication,” in *2015 IEEE/RSJ International Conference on Intelligent Robots and Systems (IROS)*, 2015, pp. 864–869.
- [18] F. J. Romero-Ramirez, R. Muñoz-Salinas, and R. Medina-Carnicer, “Speeded up detection of squared fiducial markers,” *Image and Vision Computing*, vol. 76, pp. 38–47, 2018. [Online]. Available: <https://www.sciencedirect.com/science/article/pii/S0262885618300799>
- [19] D. Roetenberg, H. J. Luinge, C. T. M. Baten, and P. H. Veltink, “Compensation of magnetic disturbances improves inertial and magnetic sensing of human body segment orientation,” *IEEE Transactions on Neural Systems and Rehabilitation Engineering*, vol. 13, no. 3, pp. 395–405, 2005.
- [20] M. M. Rahman, R. Ikeura, and K. Mizutani, “Control characteristics of two humans in cooperative task,” in *Smc 2000 conference proceedings. 2000 IEEE international conference on systems, man and cybernetics. 'cybernetics evolving to systems, humans, organizations, and their complex interactions' (cat. no.0, vol. 2, 2000, pp. 1301–1306 vol.2*.
- [21] A. Mörtl, M. Lawitzky, A. Kucukyilmaz, M. Sezgin, C. Basdogan, and S. Hirche, “The role of roles: Physical cooperation between humans and robots,” *The International Journal of Robotics Research*, vol. 31, no. 13, pp. 1656–1674, Nov. 2012.
- [22] D. Feth, R. Groten, A. Peer, S. Hirche, and M. Buss, “Performance related energy exchange in haptic human-human interaction in a shared virtual object manipulation task,” in *World Haptics 2009 - Third Joint EuroHaptics conference and Symposium on Haptic Interfaces for Virtual Environment and Teleoperator Systems*, 2009, pp. 338–343.
- [23] C. Murchison and H. Banister, *A Handbook of General Experimental Psychology*. Clark University Press, 1934. [Online]. Available: <https://books.google.com/books?id=aEUczQEACAAJ>
- [24] D. L. Woods, J. M. Wyma, E. W. Yund, T. J. Herron, and B. Reed, “Factors influencing the latency of simple reaction time,” *Frontiers in Human Neuroscience*, vol. 9, Mar. 2015.